Design Optimization of Reflective Polarizers for LCD Backlight Recycling

Yan Li, Thomas X. Wu, *Senior Member, IEEE*, and Shin-Tson Wu, *Fellow, IEEE*

***Abstract*—We systematically study and optimize the design of multilayer birefringent reflective polarizers for recycling the backlight of liquid crystal displays. Factors affecting the Bragg reflection are analyzed in detail, including number of layers for establishing Bragg reflection, refractive index difference, effective refractive index, and thickness ratio. Different methods for achieving broadband reflection are investigated, so that the reflective polarizer could cover the entire visible wavelengths and a large incident angle. In addition, the effects of material dispersion on the device design are analyzed.**

***Index Terms*—Birefringent, liquid crystal display (LCD), multilayer, polymer, reflective polarizer.**

I. Introduction

In a conventional liquid crystal display (LCD) system, two crossed absorption-type linear sheet polarizers are commonly used in order to achieve a high contrast ratio [1]. The bottom polarizer absorbs more than half of the unpolarized backlight, because only the light polarized along the transmission axis could pass through. Low optical efficiency implies to high power consumption. How to enhance the energy efficiency of LCDs is an urgent issue.

Backlight recycling using a reflective polarizer improves the optical efficiency by $\sim$60% [2]. When the unpolarized backlight hits the reflective polarizer, one linear polarization (say, p-wave) will pass through while the other component (s-wave) will be reflected back for recycling. After hitting the rough surface of the diffuser, the s-wave is depolarized. Upon reflection from the diffusive reflector, the p-wave is transmitted and s-wave reflected again for recycling. In each cycle, about half of the incident light passes through the polarizer. After 3–5 cycles, about 50%–60% of the s-wave is converted to p-wave.

Several types of reflective polarizers have been developed. **1)** Polarizing beam splitter that is based on Brewster's angle; this method works well only for a small range of incident angle. **2)** Nano-wire grid [3]–[6]: based on effective refractive index theory, the effective refractive index in one direction has a large imaginary part and works as a metal mirror if the thickness is properly controlled, while in the other direction, the effective index is like a dielectric material and light polarized in that direction could transmit through with little absorption loss. The fabrication of large-panel nano-wire grid polarizer is still challenging at present as it is waiting for the nano-imprinting technique to mature. **3)** Multilayer reflective polarizer. This device is first introduced by 3M, better known as DBEF (Dual Brightness Enhancement Film) [7], [8]. DBEF provides a mechanism to recycle the backlight before it enters the LCD panel resulting in a big improvement in optical efficiency. The DBEF manufacturing technology is mature and is commonly used in commercial products, especially for those battery-powered mobile displays, such as cell phones and notebook computers. However, the design process of DBEF is not systematically described in literature.

In this paper, we systematically study the properties of Bragg reflection of multilayer birefringent polarizer and optimize its design methods to achieve a high reflectance over the entire visible wavelengths and large incident angle. All the factors affecting Bragg reflection are investigated, e.g., the number of periodic layers, refractive index difference, effective refractive index, and optical thickness ratio. In order to broaden the bandwidth, methods such as multi-stacking of uniform layer thickness and gradient layer thickness are investigated. Also, the effects of oblique angle incidence and materials refractive index dispersion are analyzed.

II. Device Structure and Working Principle

Fig. 1 shows the device structure of a multilayer birefringent reflective polarizer consisting of hundreds of alternative layers (materials 1 and 2). Material 1 is an isotropic polymer, while material 2 is a positive birefringence uniaxial polymer. There is a large refractive index difference between the two materials in x axis, while in the other two axes (y and z) their refractive indices are substantially matched. Here z represents the light propagating direction perpendicular to the layers. Meanwhile, the optical thickness of each layer is controlled to be a quarter of a particular wavelength. Therefore, Bragg reflection could be established for the polarization component along x-axis. For the convenience of discussion, let us call it x-polarization. For y-polarization, it sees a thick slab with uniform refractive index and is transmitted with high efficiency. Our design goal is to optimize the reflectance for x-polarization and optimize the transmittance for y-polarization.

III. Bragg Reflection of Uniform Periodic Layers

In the following sections, we use 4×4 matrix method [9], [10] to analyze the reflectance of x-polarization (the direction

Manuscript received May 11, 2009; revised June 25, 2009. Current version published August 05, 2009. This work was supported by Chi-Mei Optoelectronics Corporation (Taiwan).

Y. Li and S.-T. Wu are with the College of Optics and Photonics, University of Central Florida, Orlando, FL 32816 USA (e-mail: yanli@mail.ucf.edu; yanli@creol.ucf.edu; swu@mail.ucf.edu).

T. X. Wu with School of Electrical Engineering and Computer Science, University of Central Florida, Orlando, FL 32816 USA (e-mail: tomwu@mail.ucf.edu).

Color versions of one or more of the figures in this paper are available online at http://ieeexplore.ieee.org.

Digital Object Identifier 10.1109/JDT.2009.2027033

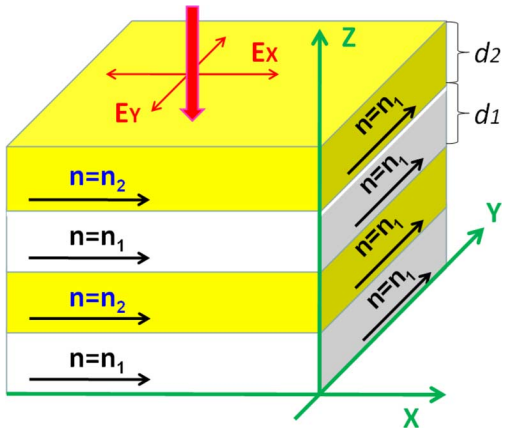

Fig. 1. The structure of a multilayer birefringent polymeric reflective polarizer.

in which refractive indices are mismatched). In our simulation, we choose material 1 (isotropic) with a refractive index of 1.57 and material 2 (uniaxial) with $n_x = n_e = 1.82$, and $n_y = n_z = n_o = 1.57$ at $\lambda = 0.55$ μm. For convenience, we designate the isotropic material's refractive index as n_1 and the uniaxial material's refractive index in x direction as n_2, as depicted in Fig. 1. According to the extended Cauchy model [11], [12], the refractive indices n_1 and n_2 decrease as the wavelength increases:

$$n_{1,2} = A_{1,2} + B_{1,2}/\lambda^2 + C_{1,2}/\lambda^4 \tag{1}$$

where $A_{1,2}$, $B_{1,2}$ and $C_{1,2}$ are the fitting parameters. For low birefringence materials, the third term is too small and can be neglected [13]. It is known that polymers and liquid crystals have similar dispersion behaviors as long as their core structures are similar [14]. Based on the data reported in [15], we found $A_1 = 1.5519$, $B_1 = 0.0036$ μm^2, $C_1 = 0.00049$ μm^4, and $A_2 = 1.74775$, $B_2 = 0.01184$ μm^2, $C_2 = 0.00303$ μm^4 at room temperature for NOA81 and BL038, respectively. We will use these dispersions for the materials 1 and 2 shown in Fig. 1.

All the structures discussed in this section consist of uniform periodic layers with $n_1 d_1 + n_2 d_2 = \lambda_B/2$, where d_1 and d_2 are the physical thicknesses of material 1 and material 2, respectively. In the following subsections, each layer has a quarter-wave optical thickness for the light polarized in x direction.

A. Number of Periodic Layers to Establish Bragg Condition

In order to establish Bragg reflection, a minimum number of periodic layers is required. Fig. 2 depicts the reflectance of x-polarization using different numbers of polymeric layers. For all cases, the central wavelength is kept the same (0.55 μm). For the case of 20 alternative layers (black curve), the maximum reflectance is only ~80%. This is because the multi-order interference is not strong enough to establish Bragg reflection due to insufficient number of layers. As the number of alternative polymer layers increases, the oscillation frequency increases, and the reflectance within the bandwidth becomes higher and flatter. The blue curve represents the simulation results for 100 layers whose reflectance reaches ~100% over the bandwidth. Although more layers lead to a sharper and more saturated Bragg reflection, it increases material cost and manufacturing

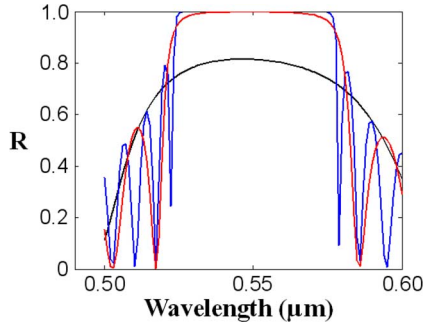

Fig. 2. Simulated reflectance (R) of x-polarization under different numbers of layers. The black curve is for 20 alternative layers, red for 50 layers, and blue for 100 layers. Here, $n_2 - n_1 = 0.25$ at $\lambda = 0.55$ μm.

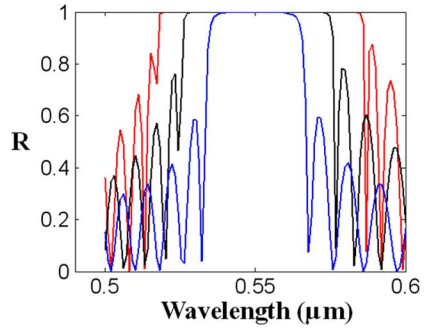

Fig. 3. Simulated reflectance for x-polarization with different Δn values. The black curve is for $\Delta n = 0.25$, blue curve for $\Delta n = 0.15$, and red curve for $\Delta n = 0.35$. In each case, there are 100 alternative layers, and the Δn values are for $\lambda = 0.55$ μm.

complexity. In Fig. 2, we also include the results of 50 layers (red color) for comparison. The results are comparable to those of 100 layers (blue color). Thus, our design strategy is to use a minimal number of layers to achieve an acceptable reflectance and bandwidth.

B. Refractive Index Difference

According to Bragg reflection, the reflection bandwidth is linearly proportional to the refractive index difference $\Delta n = n_2 - n_1$ between the two polymers employed [1]. As shown in Fig. 3, when we increase or decrease Δn, while keeping $n_{\text{eff}} = (n_1 + n_2)/2$ and λ_B (0.55 μm) unchanged, the bandwidth increases or decreases accordingly.

A large Δn helps to expand the bandwidth. However, Δn is limited by the molecular conjugation length of the employed polymers and cannot be arbitrarily increased. The red curve shown in Fig. 2, even with an aggressively high $\Delta n = 0.35$, has a bandwidth of only about 70 nm, which is still far short from covering the entire visible wavelengths. Therefore, although high Δn polymers are favorable in broadband design, by simply increasing the Δn from material side could not make the bandwidth broad enough for display applications. Other broadband device concepts need to be explored.

C. Effective Refractive Index

During our studies, we found that the effective refractive index $[n_{\text{eff}} = (n_1 + n_2)/2]$ also has some effects on the bandwidth of Bragg reflection. As shown in Fig. 4, as the effective

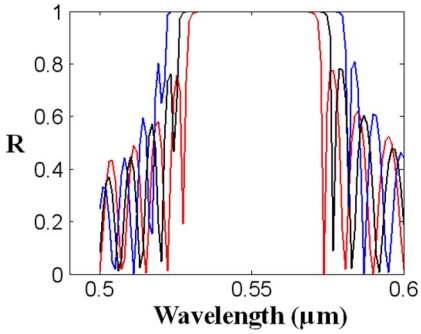

Fig. 4. Effective refractive index effect on the simulated reflectance for x-polarization. The black curve is for $n_{\text{eff}} = 1.595$, blue curve for $n_{\text{eff}} = 1.295$, and red curve for $n_{\text{eff}} = 1.895$. In each case, there are 100 alternative layers, and the n_{eff} values are for $\lambda = 0.55$ μm.

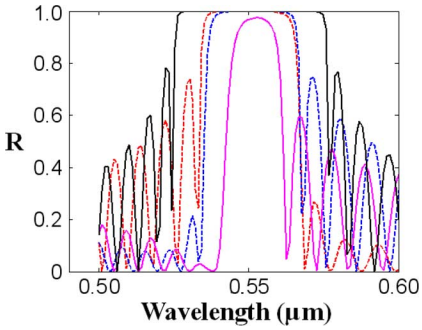

Fig. 5. Simulated reflectance of light polarized in x direction with different n_1d_1/n_2d_2 ratios. The black curve is for $n_1d_1/n_2d_2 = 1$, red for $n_1d_1/n_2d_2 = 4$, blue for $n_1d_1/n_2d_2 = 1/4$, and magenta for $n_1d_1/n_2d_2 = 1/9$. In each case, there are 100 alternative layers.

refractive index increases while keeping all other parameters ($\Delta n = n_2 - n_1$ and $\lambda_B = 0.55$ μm) fixed, the bandwidth decreases slightly. Thus, a lower refractive index leads to a broader bandwidth. One possible explanation of this phenomenon is as follows. As n_{eff} decreases, the Fresnel reflection at the first interface is reduced, so more energy is distributed among the higher order reflections. As a result, the interaction among all the reflection orders is enhanced.

D. Optical Thickness Ratio

In above discussions, the optical thickness for each layer of material 1 and material 2 is the same, i.e., $n_1d_1 = n_2d_2 = \lambda_B/4$. But in device fabrication, a large tolerance in layer thickness is highly desirable. We also studied how the layer thickness variation affects the performance of the reflective polarizer. Fig. 5 shows the simulation results if the optical thickness is not exactly the same for the two materials employed. From Fig. 5, we found that the more different n_1d_1 and n_2d_2 are, the narrower the bandwidth becomes and the lower the reflectance. Meanwhile, we also noticed that one side of oscillation is suppressed when $n_1d_1 \neq n_2d_2$. If $n_1d_1 > n_2d_2$ (red curve), then the oscillation loops on the long wavelength side is suppressed, and vise versa. Thus, the optimal condition to design a broadband reflective polarizer is to keep the optical thickness of the two materials as close as possible.

IV. Broadband Bragg Reflection

Most of the backlight used in display systems is unpolarized white light with Lambertian emission distribution. Although some light turning films, such as 3M's brightness enhancement film [16], can concentrate a Lambertian light to a $\pm 40^{\circ}$ cone, it is still desirable that the broadband reflective polarizer can accommodate a large acceptance angle. Blue shift is a common phenomenon for Bragg reflection. As the incident angle increases, the reflection spectrum shifts toward a shorter wavelength [1].

To enhance the recycling efficiency in a display system, the reflectance of x-polarization should be as high as possible. As shown in Fig. 6, each time one half of the unpolarized light (the x polarization component) transmits thru the polarizer, and another half is reflected for recycling. Thus, the total energy that gets into LCD panel is the sum of the subsequently transmitted light, expressed as:

$$T_{total} = T_1 + T_2 + T_3 + \cdots T_i + \cdots \tag{2}$$

where T_i, is the transmitted light at the i-*th* incidence. To be noticed, here only the light polarized in y-direction counts in the output side, for the x-polarization leakage would finally be absorbed by the bottom linear polarizer (not shown in the figure) of the LCD panel. Thus, T_i could be expressed as

$$T_i = \frac{1}{2}T_y \cdot \left[\frac{1}{2}(2 - T_x - T_y)T_d\right]^{i-1} \tag{3}$$

where T_x is the transmittance of the reflective polarizer for the light polarized in x-direction and T_y is the transmittance for the light polarized in y-direction. The $(1/2)T_y$ term is the ratio of the exiting y-polarization to the unpolarized incident light each time. The $(1/2)(2-T_x-T_y)$ term is the ratio of reflected energy each time (dominated by x polarization) and T_d is the efficiency of the diffusive reflector. Thus,

$$\begin{aligned} T_{\text{total}} &= \sum_{i=1}^{\infty} T_i = \lim_{N\to\infty} \frac{1}{2}T_y \cdot \frac{1 - \left[\frac{1}{2}(2 - T_x - T_y)T_d\right]^{N-1}}{1 - \frac{1}{2}(2 - T_x - T_y)T_d} \\ &= \frac{1}{2}T_y \cdot \frac{1}{1 - \frac{1}{2}(2 - T_x - T_y)T_d} \end{aligned} \tag{4}$$

According to our simulation, $T_y \sim 90\%$ and the T_d of 3M's ESR (Enhanced Specular Reflector) is more than 98.5%. If $T_x = 5\%$, then T_{total} is as high as 93.2%, assuming the reflective polarizer has a negligible absorption loss. By contrast, the maximum transmittance of two conventional absorptive linear polarizers is only ~40%. This implies if we can design a reflective polarizer with 95% reflectance, after perfect recycling the optical efficiency would be doubled as compared to that without using a reflective polarizer. But in reality, there are always some absorption and scattering losses associated with the optical films, such as diffusers. Thus, the recycling efficiency drops to ~60%.

As mentioned in Section III, it is difficult to achieve broad bandwidth by using a uniform-thickness stacking, even when its number of layers, refractive index difference, effective refractive index, and thickness ratio are practically optimized. In order to broaden the bandwidth of Bragg reflection,

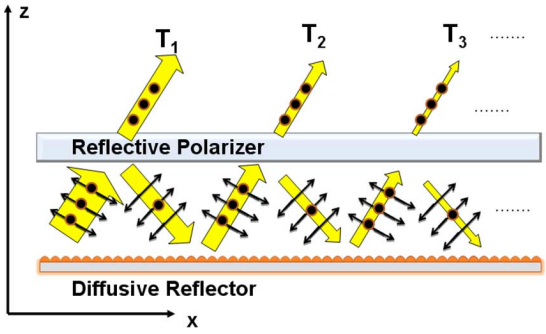

Fig. 6. The diagram showing multi-step backlight recycling. Ti is the light transmitted through the reflective polarizer at the ith cycle.

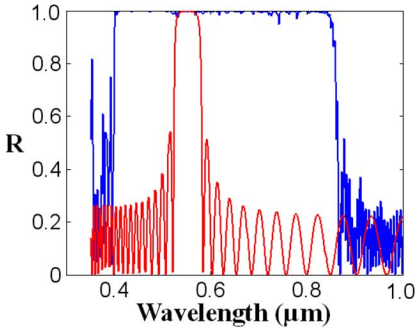

Fig. 7. Simulated reflectance of stacked structures. The blue curve is for a multi-stack film, whose central wavelengths are 0.42, 0.46, 0.50, 0.55, 0.60, 0.65, 0.70, 0.76, and 0.82 μm. The red curve is for a single-stack film with central wavelength at 0.55 μm. Each stack has 50 alternative layers, so the blue curve consists of 450 layers.

multi-stacking of uniform layer thickness and gradient layer thickness approaches, similar to those of cholesteric liquid crystals [17], are investigated.

A. Multi-Stacking Approach

In this approach, each stack consists of 50 alternative layers with equal optical thickness ($n_1d_1 = n_2d_2 = \lambda_B/4$) and covers a bandwidth of less than 100 nm, centered at λ_B. When we want to shift the bandwidth, which means changing the targeted central wavelength λ_B, we simply scale the thicknesses of all the layers within the stack correspondingly. In this multi-stacking design, we choose different λ_B's for different stacks, so that their bandwidths could be shifted in such a way that each stack's bandwidth slightly overlaps with its neighbors'. Thus, their bandwidths could be superimposed and the total bandwidth is most effectively extended.

Fig. 7 demonstrates the expanded bandwidth achieved by multi-stacking method compared to the single stack. Here, the central wavelength of the multi-stacks is chosen to be $\lambda_B = 0.42, 0.46, 0.5, 0.55, 0.6, 0.65, 0.7, 0.76,$ and 0.82 μm, respectively, and 0.55 μm for the single-stack. Thus, the total layer count for the 9-stacked film is 450. The step of increasing λ_B should be carefully controlled. If it is too small, the bandwidth of each stack will overlap too much so that more stacks than necessary are needed. On the other hand, if it is too large, they are too far apart and some regions near the boundaries will not be covered, which leads to a discontinuous spectrum. In our design, the bandwidth covers from 0.4 to 0.85 μm. We

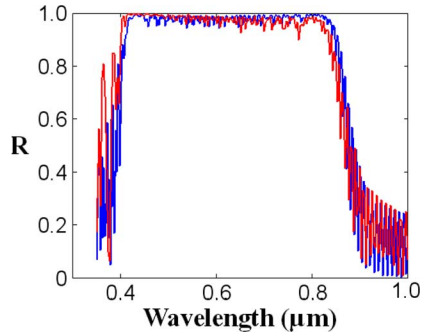

Fig. 8. Simulated reflectance for x-polarization using linear (blue) and exponential (red) gradient thickness distributions. Both have 300 alternative layers and $\Delta n = 0.25$.

intentionally overdesign it for the longer wavelength side in order to take blue shift at oblique incidence into consideration.

B. Gradient-Thickness Approach

Another approach to achieve broadband reflection is to use alternative pairs with gradient thicknesses. Here, we tried two approaches: linear gradient and exponential gradient. Their thickness gradients in z direction are given by

$$\begin{aligned} \text{Linear} &: 4\mathrm{n}_i d_i = \lambda_{Bi} = 0.4 + i/N \cdot 0.4 \\ \text{Exponential} &: 4n_i d_i = \lambda_{Bi} = 0.4 * \exp\left(i/N \cdot (0.8/0.4)\right). \end{aligned} \quad (5)$$

Fig. 8 shows the simulated results using linear gradient thickness (blue curve) and exponential gradient thickness (red curve). In both cases, the total number of layers is 300 and the bandwidth is from 0.40 to 0.85 μm. From Fig. 8, the linear gradient approach has a uniform reflectance over the entire bandwidth, while the exponential gradient one exhibits a superior performance at shorter wavelength but inferior at longer wavelength. Thus, the linear gradient thickness approach is more favorable than the exponential one for broadband design. Both gradient approaches work better than the multi-stacking one because fewer layers are needed.

C. Angular Dependence

For a wide-view LCD, the backlight is heavily diffused before reaching the reflective polarizer, i.e., light randomly comes in all directions. Therefore, the reflective polarizer needs to be designed not only for normal but also for oblique incidences. Fig. 9 compares the performances of the reflective polarizer at normal (black curve), 30° (blue), 60° (red), and 85° (gray) incident angles. We find that as incident angle increases, the bandwidth becomes narrower and the whole band moves towards the shorter wavelength side. This is because the effective optical thickness decreases at an oblique incidence:

$$n_i d_i \cos\left[\sin^{-1}(\sin\theta/n_i)\right] = \lambda_B/4 \quad (6)$$

where θ is the incident angle in air. Consequently, Bragg wavelength λ_B is reduced and the corresponding bandwidth decreased [1]. From Fig. 9, the reflectance remains quite high in the entire visible region even at 85° incident angle. So by stretching the bandwidth into near IR region (from 0.4 μm to 0.85 μm) at normal incidence, the reflective polarizer can still

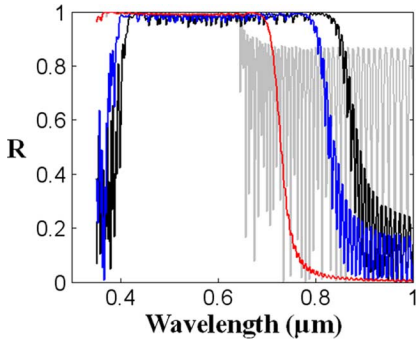

Fig. 9. Incident angle dependent reflection spectra of a reflective polarizer with linear gradient thickness. Black curve is for normal incidence; blue, red, and gray curves are for 30°, 60°, and 85° oblique incidences, respectively.

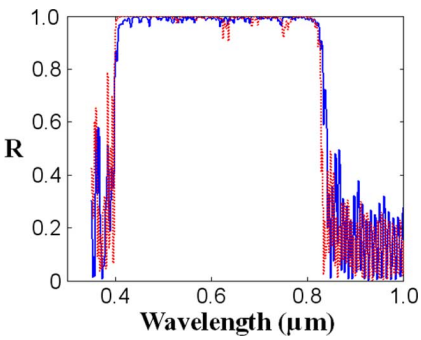

Fig. 10. Simulation results without (blue) and with (red) consideration of material dispersions.

function well in the visible region even at a large incident angle. This feature is practically important for a wide-view LCD.

D. Material Dispersion

According to (1), the refractive index is dependent on the wavelength. In designing a broadband reflective polarizer, we must take the dispersive property of materials into account. Otherwise, even an ideally designed reflective polarizer would not function properly for practical applications. In Fig. 10, we compare the reflectance of a reflective polarizer with (red curve) and without (blue curve) considering the material dispersion. The blue curve seems to have uniform reflectance over the entire visible region. However, these data do not include the refractive index dispersion and are not accurate. The actual results are shown by the red curve, where some bands do not overlap too well, especially in the longer wavelength side. This is because for real dispersive materials, Δn decreases as the wavelength increases. Therefore, the actual bandwidth for longer wavelength is a little bit narrower than expected for non-dispersive materials. As a result, more stacks would be needed for real materials so that the bands would be close enough to cover their boundaries.

V. Conclusion

We have used 4 × 4 matrix method to study the Bragg reflection of a birefringent reflective polarizer. By analyzing all the factors that affect Bragg reflection, we found that 1) a minimum number of alternative layers is needed to establish Bragg reflection, 2) larger refractive index difference, low effective index, and equal optical thickness are favorable for broadening the reflection bandwidth. In order to make the reflective polarizer suitable for display applications, two approaches for achieving broadband Bragg reflection are analyzed: 1) Multi-stack method, and 2) Gradient-thickness methods. Both of them could extend the bandwidth to cover the entire visible range, but linear gradient method stands out, with fewer layers and reasonably good performance. Also, the effects of oblique incidence and material dispersion are investigated.

References

[1] D. K. Yang and S. T. Wu, *Fundamentals of Liquid Crystal Devices*. Hoboken, NJ: Wiley, 2006.
[2] G. R. Bird and M. Parrish, Jr., "Wire grid as a near-infrared polarizer," *J. Opt. Soc. Am.*, vol. 50, pp. 886–891, 1960.
[3] J. Wang, F. Walters, X. Liu, P. Sciortino, and X. Deng, "High-performance, large area, deep ultraviolet to infrared polarizers based on 40 nm line/78 nm space nanowire grids," *Appl. Phys. Lett.*, vol. 90, pp. 061104-1–061104-3, 2007.
[4] S. H. Kim, J. D. Park, and K. D. Lee, "Fabrication of a nano-wire grid polarizer for brightness enhancement in liquid crystal display," *Nanotechnology*, vol. 17, pp. 4436–4438, 2006.
[5] Z. Ge and S. T. Wu, "Nanowire grid polarizer for energy efficient and wide-view liquid crystal displays," *Appl. Phys. Lett.*, vol. 93, pp. 121104-1–121104-3, 2008.
[6] X. Yang, Y. Yan, and G. Jin, "Polarized light-guide plate for liquid crystal display," *Opt. Express*, vol. 13, pp. 8349–8356, 2005.
[7] M. F. Weber, C. A. Stover, L. R. Gilbert, T. J. Nevitt, and A. J. Ouderkirk, "Giant birefringent optics in multilayer polymer mirrors," *Science*, vol. 287, pp. 2451–2456, 2000.
[8] J. M. Jonza, M. F. Weber, A. J. Ouderkirk, and C. A. Stover, "Polarizing Beam-Splitting Optical Component," U.S. Patent, 5962114, October 5, 1999.
[9] D. W. Berreman, "Optics in stratified and anisotropic media: 4 × 4 matrix formulation," *J. Opt. Soc. Am.*, vol. 62, pp. 502–510, 1972.
[10] Y. H. Huang, T. X. Wu, and S. T. Wu, "Simulations of liquid-crystal Fabry-Perot etalons by an improved 4 × 4 matrix method," *J. Appl. Phys.*, vol. 93, pp. 2490–2495, 2003.
[11] S. T. Wu, C. S. Wu, M. Warenghem, and M. Ismaili, "Refractive index dispersions of liquid crystals," *Opt. Eng.*, vol. 32, pp. 1775–1780, 1993.
[12] J. Li and S. T. Wu, "Extended Cauchy equations for the refractive indices of liquid crystals," *J. Appl. Phys.*, vol. 95, pp. 896–901, 2004.
[13] J. Li and S. T. Wu, "Two-coefficient Cauchy model for low birefringence liquid crystals," *J. Appl. Phys.*, vol. 96, pp. 170–174, 2004.
[14] S. T. Wu, "Phase-matched compensation films for liquid crystal displays," *J. Materials Chem. Phys.*, vol. 42, pp. 163–168, 1995.
[15] J. Li, G. Baird, Y. H. Lin, H. Ren, and S. T. Wu, "Refractive-index matching between liquid crystals and photopolymers," *J. Soc. Info. Display*, vol. 13, pp. 1017–1026, 2005.
[16] R. C. Allen, L. W. Carlson, A. J. Ouderkirk, M. F. Weber, A. L. Kotz, T. J. Nevitt, C. A. Stover, and B. Majumdar, "Brightness Enhancement Film," U.S. Patent, 6760157, July 6, 2004.
[17] Q. Hong, T. X. Wu, and S. T. Wu, "Optical wave propagation in a cholesteric liquid crystal using the finite element method," *Liq. Cryst.*, vol. 30, pp. 367–375, 2003.

Yan Li received the M.S. degree in optics from Zhejiang University (ZJU) in 2007, and is currently working toward her Ph.D. degree at the College of Optics and Photonics, University of Central Florida, Orlando.

Her current research interests include energy conservation and fast respond time in LCDS, and transflective LCDs.

Thomas X. Wu (S'96–M'98–SM'02) received the Ph.D. degree in electrical engineering from the University of Pennsylvania in 1999.

In the fall of 1999, he joined the School of Electrical Engineering and Computer Science, University of Central Florida (UCF) as an assistant professor. He was promoted to associate professor with tenure in 2005. He specialized in theoretical and computational electromagnetics and physics. He has been working on the modeling of liquid crystal display and photonic devices since 2001.

Prof. Wu was chairman of IEEE Orlando Section in 2004. He was awarded Distinguished Researcher of the Department of Electrical and Computer Engineering in 2003, Distinguished Researcher of College of Engineering and Computer Science in 2004, and University Research Incentive Award in 2005. Prof. Wu is also an outstanding teacher at the university. He was awarded Excellence for Undergraduate Teaching Award from the School of Electrical Engineering and Computer Science in January 2006, and Excellence for Undergraduate Teaching Award from the College of Engineering and Computer Science in February 2006. He was awarded Excellence for Graduate Teaching Award from the School of Electrical Engineering and Computer Science in January 2007, and the University Teaching Incentive Award in May 2007.

Shin-Tson Wu (M'98-SM'99-F'04) received the B.S. degree in physics from National Taiwan University, and the Ph.D. degree from the University of Southern California, Los Angeles.

He is a PREP professor at College of Optics and Photonics, University of Central Florida (UCF). His studies at UCF concentrate in liquid crystal displays, liquid crystal materials, optical communications, photonic crystal fibers, and bio-photonics. Prior to joining UCF in 2001, he worked at Hughes Research Laboratories, Malibu, CA, for 18 years. He has co-authored 5 books: Introduction to Flat Panel Displays (Wiley, 2008, with J. H. Lee and D. N. Liu), Fundamentals of Liquid Crystal Devices (Wiley, 2006, with D. K. Yang); Introduction to Microdisplays (Wiley, 2006, with D. Armitage and I. Underwood), Reflective Liquid Crystal Displays (Wiley, 2001, with D. K. Yang) and Optics and Nonlinear Optics of Liquid Crystals (World Scientific, 1993, with I. C. Khoo), 6 book chapters, over 300 journal publications, and more than 55 issued patents.

Dr. Wu is a recipient of SPIE G. G. Stokes award and SID Jan Rajchman prize. He is a Fellow of the Society of Information Display (SID), Optical Society of America (OSA), and SPIE.